agriculture

MDPI

Article

Optimal Pumping Flow Algorithm to Improve Pumping Station Operations in Irrigation Systems

Enrique Bonet * and María Teresa Yubero

Department of Mining, Industrial and ICT Engineering, Universitat Politécnica de Catalunya (UPC), Les Bases Avenue 61-73, 08242 Manresa, Spain; maria.teresa.yubero@upc.edu
* Correspondence: enrique.bonet@upc.edu

Abstract: In Spain, irrigated agriculture is the most water-intensive sector, consuming around of 80% of water resources. Moreover, irrigation water distribution systems are the infrastructure by which one-third of water resource losses take place. Monitoring and controlling operations in irrigation canals are essential for mitigating leakages and water waste in operational actions. On the other hand, energy consumption by agriculture is around 5% of usage in developed countries and even higher in undeveloped countries. Although it is a small part of the total energy supply for a country, energy waste reduces the competitiveness of the agriculture sector, which continually reduces profit margins in an economic sector with very low profit margins already. The tool developed in this paper aims to increase the efficiency of water and energy management in the agricultural sector and is included in an overall control diagram for scheduled irrigation management. This tool, the optimal pumping flow (OPF algorithm), optimizes the pumping flow from the irrigation canal to the irrigation reservoir in terms of water level at the canal and reservoir, crop flow demand, system constraints, and energy prices. Regarding the results, the OPF algorithm can calculate the optimum pumping operations, being able to optimize water resource usage and energy expenses by ensuring that the water level at reservoirs remains within a specified range and that pump flow never exceeds a threshold. Further, it allows for the management of pump operations outside of peak hours. On the other hand, the OPF algorithm is also integrated into the overall control diagram in a second test. Here, the OPF algorithm collaborates with a control canal algorithm such as the GoRoSo algorithm to optimize canal gates and pump operations, respectively. In this scenario, OPF reduces cumulative energy expenses by 58% compared to the scenario where the pump station operates only when the reservoir water level is below a certain threshold.

Keywords: agricultural demands; irrigation canal control; pump flow optimization; open channel flow; optimization algorithms

check for updates

Citation: Bonet, E.; Yubero, M.T. Optimal Pumping Flow Algorithm to Improve Pumping Station Operations in Irrigation Systems. *Agriculture* **2024**, *14*, 463. https://doi.org/10.3390/agriculture14030463

Academic Editors: Claudia Di Bene, Valentina Baratella and Silvia Vanino

Received: 5 February 2024
Revised: 28 February 2024
Accepted: 5 March 2024
Published: 12 March 2024

Copyright: © 2024 by the authors. Licensee MDPI, Basel, Switzerland. This article is an open access article distributed under the terms and conditions of the Creative Commons Attribution (CC BY) license (https://creativecommons.org/licenses/by/4.0/).

1. Introduction

As is well known, water and energy are scarce resources. On planet Earth, 97.6% of water is found in seas and oceans, while the remaining 2.4% is freshwater, which is distributed as follows: according to Gleick Peter Gilbert F. [1], 1.9% of this total is in glaciers and polar ice caps, 0.5% is groundwater, and 0.02% is in surface water (rivers, lakes, reservoirs, etc.), as shown in Figure 1. It is estimated that only 0.025% of the total water on Earth is drinkable. Global water use has multiplied sixfold in the last 100 years and continues to increase by 1% annually due to population growth, economic development, and consumption patterns. Climate change has a negative impact on the quantity and quality of available water needed to meet global human needs according to UNESCO [2]. The global population is rapidly growing, with expectations of reaching 8 billion people in 2030 and being just shy of 10 billion people in 2050 according to the United Nations [3], both of which are figures that suggest an imminent surge in global food demand.

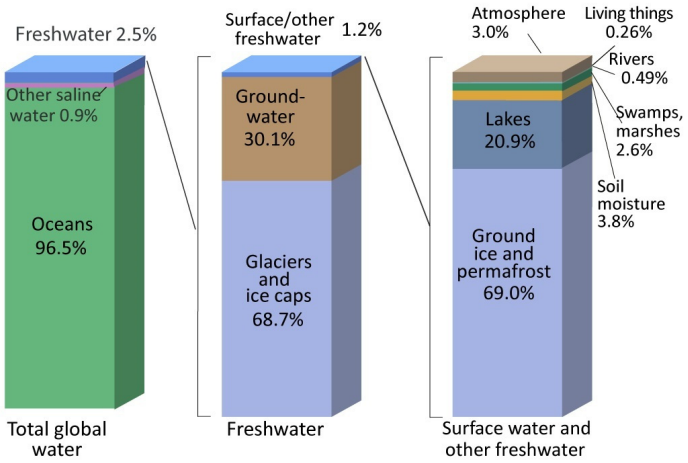


Figure 1. Global water distribution graph in [1] (data source: Igor Shiklomanov's chater "World fresh water resources" in Peter H. Gleik (editor), 1993, Water in Crisis: A guide to the World's Fresh Water Resources. (Numbers are rounded)).

Climate change manifests itself in the increased frequency and magnitude of extreme events such as heatwaves, heavy precipitation, and storms, among others. Water quality will be affected by rising temperatures, decreased dissolved oxygen levels, and consequently reduced self-purification capacity in freshwater reservoirs. Additionally, the degradation of ecosystems sensitive to climate change, such as forests and wetlands, should be taken into account. This not only leads to biodiversity losses, but also affects the services provided by these ecosystems, such as water purification, carbon storage, flood protection, and water supply according to Salimi S. et al. [4].

Optimizing energy use is a crucial goal for the agriculture sector. This is not just useful for economic sustainability but environmental sustainability as well, reducing water losses due to wrong operations and CO_2 emissions, which are quite high even now according to Romano G. et al. [5]. As shown in Figure 2, the primary energy sources in Spain were oil and natural gas, with 39.6% and 21% shares of the market in 2017, respectively. These were usually used to generate electricity according to International Energy Agency [6]. On the other hand, by 2021, wind energy had become the increasingly leading source of renewable energy. This is shown in Figure 2, which illustrates the evolution of energy sources in Spain. In 2015, 27% of consumed energy came from renewable sources, while by 2020, this percentage had increased to 31%. Therefore, there is a clear trend towards an increased consumption of renewable energy. As such, we have to reduce fuel source use but we have also to optimize energy consumption by reducing CO_2 emissions.

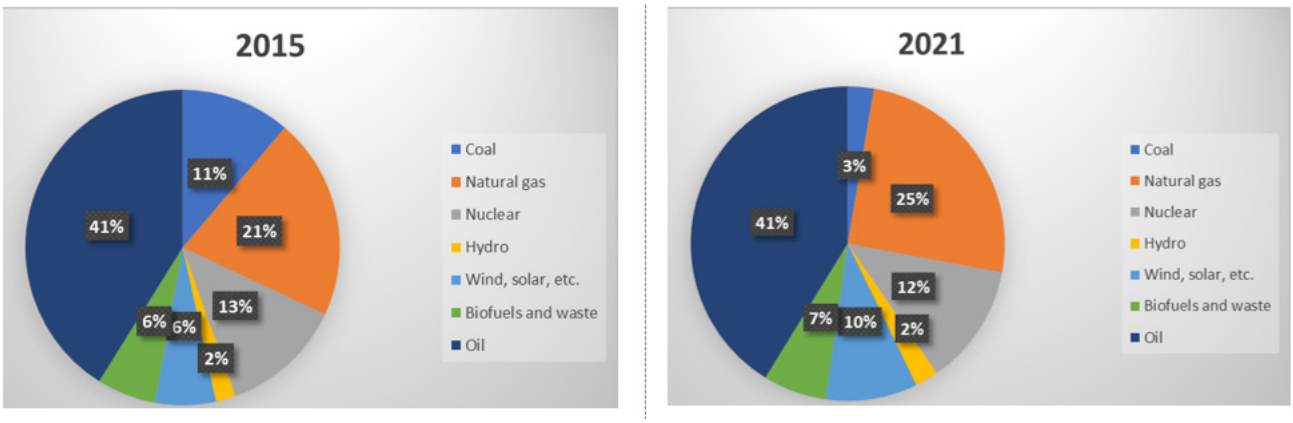


Figure 2. Energy supply distribution in Spain in 2015 and 2021 (data source: International Energy Agency: https://www.iea.org/countries/spain (accessed 12 October 2023)).

On the other hand, there exists a huge problem in agriculture surrounding increasing labour, seed, and machinery costs, as well as energy costs, during recent years. In that sense, the increase in energy cost reduces agriculture competitiveness in developed countries, as well as increasing the CO_2 emissions to the atmosphere, so all actions derived from reducing energy expenses and optimizing energy consumption in the agriculture sector are mandatory.

The energy price in Spain is established by the marginalist system. The main characteristic of this system is that the energy price is estimated by the point of intersection between demand and supply; see Peña J. I. [7]. The intersection point represents the maximum price at which the energy package is sold, so all sellers who have proposed an energy price value equal to or lower than the market price will sell their energy package. Conversely, for all buyers who have presented an offer equal to or higher than the energy market price, all offers will be accepted.

Therefore, this system encourages energy producers to adopt a strategy where their offers have the lowest possible price, contributing to a more efficient energy generation system. The greater the difference between the intersection price and the energy production cost, the higher the profit margin. This margin is often used in competitive markets where supply and demand interact to determine prices. It helps to ensure that resources are allocated efficiently and that production is aligned with consumer demand. However, in scenarios where energy demand grows rapidly and energy resources decrease, the energy price also grows sharply. Regarding the current scenario, taking action to increase water savings and optimize energy costs is crucial for the agriculture sector.

This is the reason why we developed the OPF algorithm, which optimizes pumping flow trajectories to minimize energy expenses and manage crop water demand. In the bibliography, there are several authors who have proposed various initiatives to optimize pumping stations. For instance, Alizadeh et al. [8] focused on pump type selection, capacity, number of units and energy cost, using the Lagrange method to solve the optimization problem. Instead, Müller et al. [9] employed mixed-integer nonlinear and mixed-integer linear model approaches to address the optimization problem. Additionally, other authors such as Khwaja and Tung [10] and Egito et al. [11] proposed the use of genetic algorithms to solve the optimization problem. All of them used different approaches to solve the same objective: pump station energy optimization.

In that sense, the OPF algorithm has been developed in this manuscript to optimize pumping energy expenses. However, this algorithm operates within an overall control diagram that manages an irrigation system, with each algorithm optimizing a specific process within the diagram. In this sense, the OPF algorithm optimizes pumping flow trajectories during a period of time and it is applied to join with the GoRoSo algorithm, which is a feedforward control algorithm; see Soler et al. [12], who optimized the irrigation canal gates operations. Both algorithms work together in order to optimize the irrigation system operations, i.e., canal operation using GoRoSo and pumping station operation using OPF.

In this manuscript, the OPF algorithm has been described and tested in several numerical examples to manage irrigation systems. First of all, the algorithm was tested considering two individual pumping stations supplying two separate regulatory reservoirs. In a second example, the OPF algorithm was assessed in conjunction with the GoRoSo algorithm in a more complex case based on the test cases introduced by the ASCE Task Committee on Canal Automation Algorithms, as discussed by Clemmens [13]. In both cases, the robustness and sensitivity of the algorithm were evaluated.

2. Methodology

Control systems for irrigation canals were developed to improve water infrastructure operations, with the main objective being to meet the water demands of crops for every irrigation cycle. In that sense, water demand could be planned in advance, but crop requirements are dynamic over time due to climatic factors. Therefore, the main tools of

control systems in irrigation canals should be implemented considering both steady state and unstable conditions through online and offline control algorithms. These algorithms are able to adjust operations, mainly gate operations and switching pumps on/off, based on water demands and system constraints.

All these algorithms estimate the correct operations to increase efficiency in irrigation systems, which depend on water level sensors and actuators to propose the correct operations. However, all of them must contribute synchronously to fulfill the main objective, as there are dependencies among all algorithms. Therefore, coordination of actions is mandatory for the correct development of every task to save water resources and energy, as depicted in Figure 3. For this reason, the construction of any modern online–offline predictive control model involves multiple different algorithms working together.

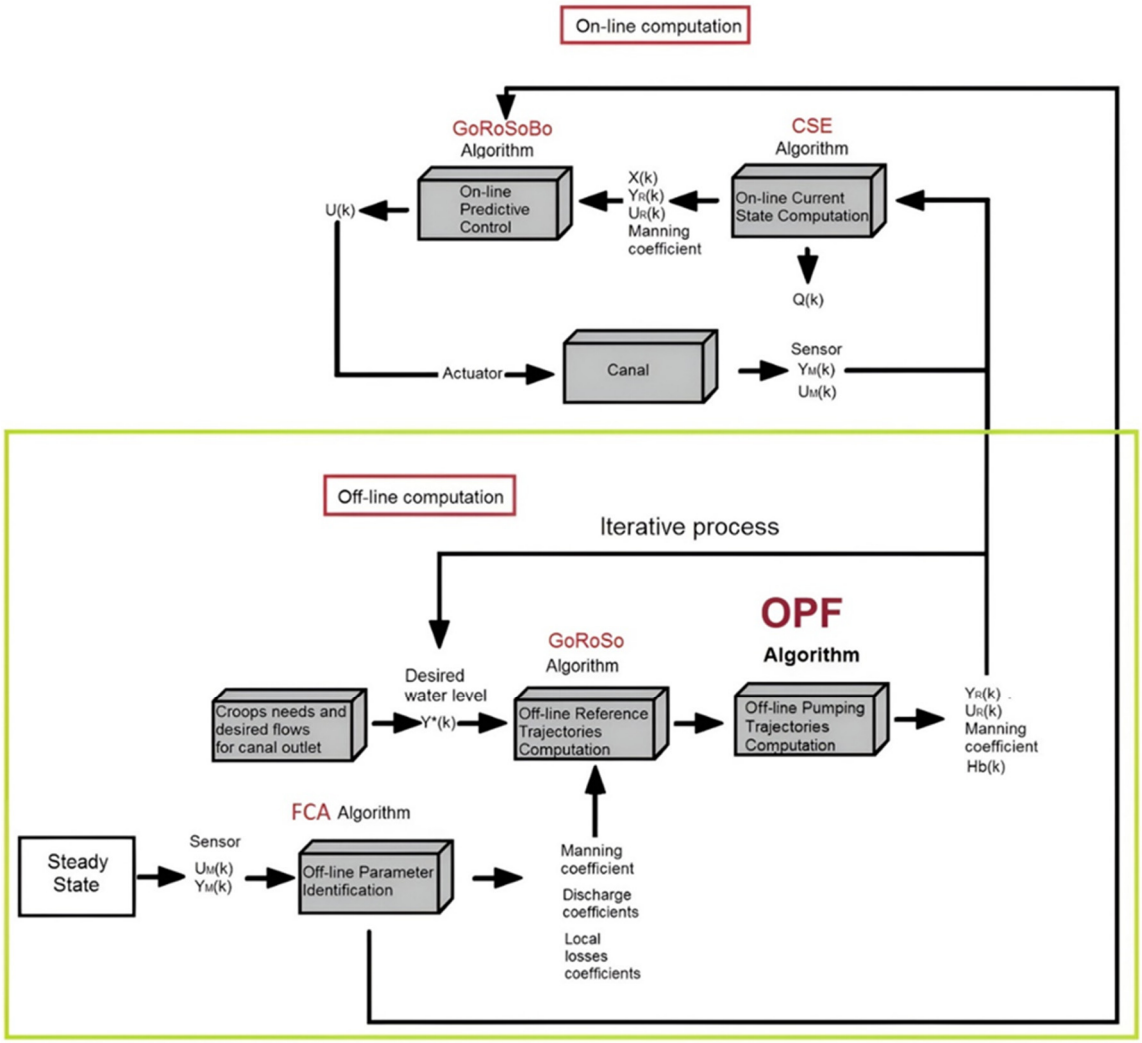


Figure 3. Overall control diagram of irrigation canal.

1. "Crop needs and desired hydrographs for canal outlets": The crop needs are estimated to obtain the water demand. In that sense, water demand is also translated to "desired water level" (Y*) at several sections of the irrigation canal.
2. "Offline computation of the reference trajectories": The desired water levels (Y*) are provided to the GoRoSo algorithm (offline reference trajectory computation), which calculates the optimum canal gate trajectory (Ur) during an irrigation period to minimize gate movements while maintaining the desired water level at specific canal sections. This is essential for diverting the correct water demand through the gravity orifice offtake, as illustrated in Figure 4. The GoRoSo algorithm is a feedforward

control algorithm that calculates the optimum canal gate trajectories in advance of the next irrigation cycle, according to Soler et al. [12].

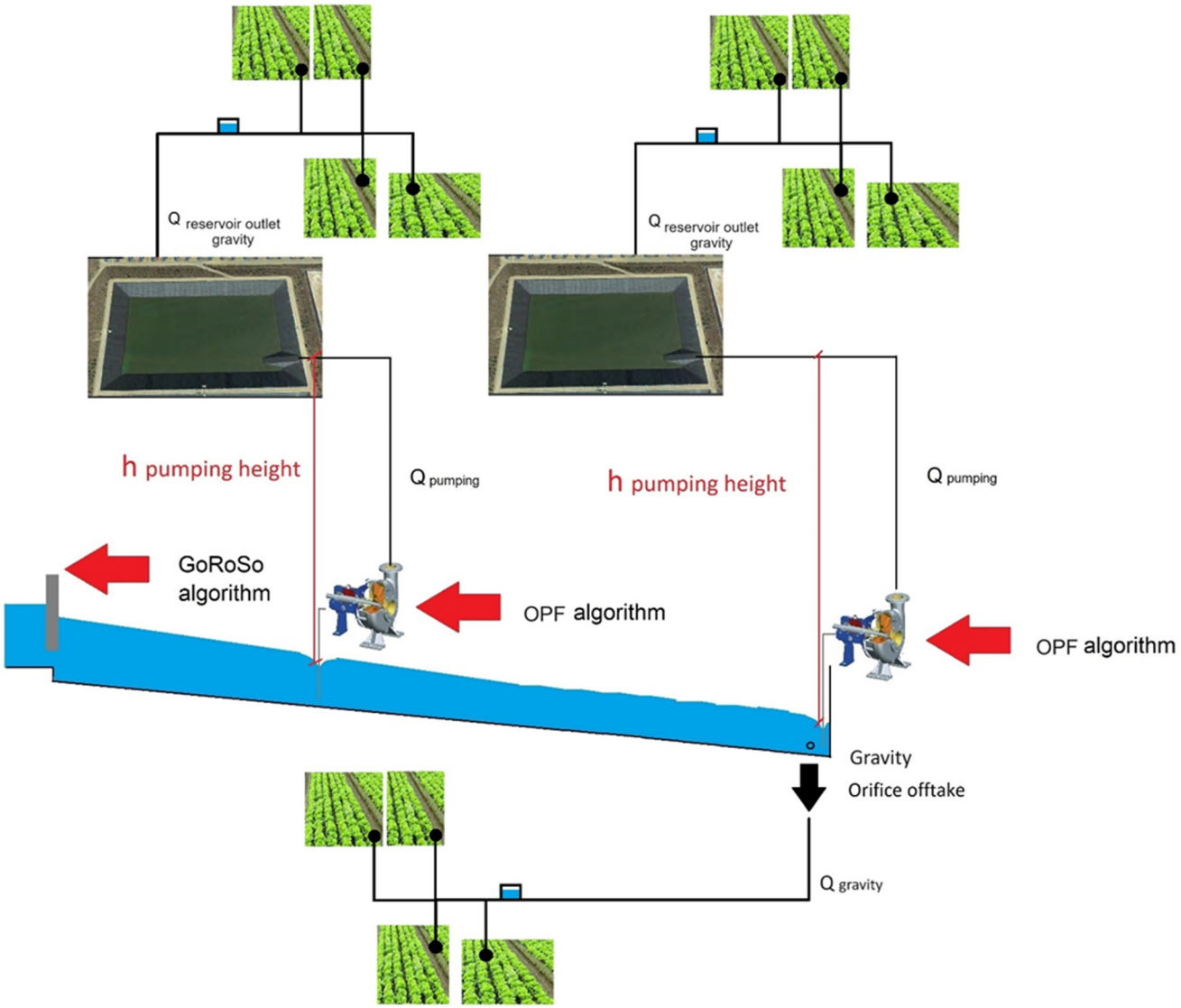


Figure 4. Simplified overall control diagram (offline computation) applied to an irrigation system.

3. "Offline parameter identification": The estimation of particular hydraulic coefficients, such as Manning coefficient or gate discharge coefficient; see the FCA algorithm (Bonet et al. [14]) or Coon W. F. [15].
4. "Offline pumping trajectory computation": A pumping station is required to supply flow from the irrigation canal to a higher regulatory reservoir. In that sense, the regulating reservoir also supplies water to irrigation crops; see Figure 4. The OPF algorithm introduced in this manuscript calculates the optimum pumping flow trajectory during a period of time in order to reduce energy consumption and expenses associated with providing for crop water demand and maintaining system requirements. Other authors have proposed different algorithms in this area such as Lindell E. et al. [16], Bohórqueza J. et al. [17], McCormick G. and Powell A R. S. [18] or Reis, A.L. [19].
5. "Online current state computation": In order to evaluate the correct behaviour of the irrigation system, it is imperative to measure the current state of the irrigation system. In this regard, all data stored in the database are crucial, such as "U" (gate position) and Y_M (measured water level), previously measured by sensors at target points in

the canal. Anomalies between the measured water level and the desired water level at target points are because of flow disturbances introduced to the system. In such circumstances, the CSE algorithm is able to estimate the flow disturbances in the canal (Bonet E. [20]), representing the real water demand in the canal. Additionally, the algorithm can determine the current hydrodynamic state of the canal, which is highly valuable in any scenario. The hydrodynamic state of a canal is defined as the velocity and water level at each cross-section of the canal.

6. "Online predictive control": In case of water anomalies regarding the irrigation system state planification, it is necessary to estimate the real water demand and the current hydrodynamic state of the canal, which are provided by the CSE algorithm. In this context, the real water demand, reference gate trajectories, and the hydrodynamic canal state are supplied to the control algorithm, known as "Online Predictive Control", which must recalculate a new gate trajectory (U) in real-time to return to the reference behaviour for a predictive horizon time period. There is an extensive bibliography of feedback control algorithms that recalculate the gate trajectories, such as those proposed by Aguilar J. V. et al. [21], Litrico et al. [22], Clemmens et al. [23], GoRoSoBo (Bonet E. et al. [24]), and Wahlin et al. [25].

In order to introduce the OPF algorithm in the overall control diagram of an irrigation canal, it would be useful to divide the diagram into two parts: the online and the offline computation, although the offline computation module (green box in Figure 3) could be applied independently of online modules. This paper is only focused on the offline computation module because the OPF algorithm was exclusively applied for planning tasks. Specifically, the OPF algorithm will support the operational tasks by estimating the pumping operations for a planned irrigation period (not in real-time). The offline module is applied for operational purposes in a planning mode, whereas the online module is only applied in the case of a highly dynamic system with unknown processes.

The main processes developed by each algorithm in the online computations are beyond the scope of this manuscript but can be reviewed in Bonet E. [24].

Regarding offline computation processes, the sequential processes included in this manuscript are as follows: the offline computation module starts once offline parameter identification has estimated the correct hydraulic coefficients, so a feedforward control algorithm, such as GoRoSo, calculates the optimum canal gate trajectories for a horizon period of time (also called irrigation cycle) in order to reach the irrigation management objectives, i.e., water level targets at specific canal sections, in order to supply the correct water flow demand at the gravity orifice offtake; see Figure 4. GoRoSo also considers pumping flow trajectories at specific canal sections (water flow to regulatory reservoirs above the irrigation canal) for a horizon period of time. Once GoRoSo finishes all calculations, the output information is shared with the OPF algorithm, which recalculates the optimum pumping flow trajectories regarding new canal water levels, system behaviour and requirements (i.e., regulation reservoirs, pipelines and irrigation canal) and crop demand (located further up than irrigation canal), minimizing energy consumption and expenses. An iterative procedure is applied to the algorithm to achieve a convergence criterion previously defined to obtain the optimum solution; see Figure 3.

In that sense, the OPF algorithm is working together with GoRoSo in an iterative process in order to estimate the optimum pumping flow trajectories and canal gate trajectories, respectively, for planning and managing the irrigation system properly.

The development of the GoRoSo algorithm is beyond the scope of this paper, which can be reviewed in Soler et al. [11]. In this paper, we focus on offline pumping trajectory computation solved by the OPF algorithm. The optimum pumping flow trajectory is crucial for any pumping station and irrigation system management due to high energy expenses as well as pumping station maintenance costs. In this sense, higher energy expenses affect the farmers' P&L, reducing the irrigation system's competitiveness.

In conclusion, the OPF algorithm presented in this manuscript is conceived as an algorithm included in the "offline pumping trajectory computation" process at the overall

control diagram of an irrigation system. The algorithm estimates the optimum pumping flow trajectories, reducing energy expenses and providing for the crop water demand, maintaining system requirements for a regulated period of time.

The OPF solves an optimization problem implemented as a constrained linear optimization problem using the SLSQP method (sequential least square programming), whose solution is the pumping flow trajectories associated with a minimum energy expense.

2.1. SLSQP (Sequential Least Square Programming)

SLSQP is designed to solve non-linear problems efficiently. Specifically, this method solves the system by performing a quadratic approximation of the objective function and the constraints, thus avoiding the direct calculation of the Hessian matrix. The steps involved in the optimization of the resolution to the problem are as follows:

Consider a nonlinear optimization problem from Equation (1)

$$\begin{array}{c} \min\limits_{x} f(x_k) \\ Inequality\ constraints:\ h(x) \geq 0 \\ Equality\ constraints:\ g(x) = 0 \end{array} \tag{1}$$

The Lagrangian function of this problem is as follows:

$$L(x, \lambda, \sigma) = f(x) - \lambda h(x) - \sigma g(x) \tag{2}$$

where λ and σ are the Lagrange multipliers (scalars).

On the other hand, we can evaluate the incremental solution as follows:

$$\begin{array}{c} s(x_k + \Delta x) = s(x_k) + s'(x_k)\Delta x + \frac{1}{2}s''(x_k)\Delta x^2 \\ \frac{ds(x_k+\Delta x)}{dx} = \frac{d}{dx}\left(s(x_k) + s'(x_k)\Delta x + \frac{1}{2}s''(x_k)\Delta x^2\right) = s'(x_k) + s''(x_k)\Delta x = 0 \\ \Delta x = \frac{s'(x_k)}{s''(x_k)} = x_{k+1} - x_k \end{array} \tag{3}$$

Applying the Newton standard method to optimization problems (1) and (2) considering the incremental solution approach (3),

$$\begin{bmatrix} x_{k+1} \\ \lambda_{k+1} \\ \sigma_{k+1} \end{bmatrix} = \begin{bmatrix} x_k \\ \lambda_k \\ \sigma_k \end{bmatrix} - \underbrace{\begin{bmatrix} \nabla^2_{xx} L & \nabla \mathrm{h} & \nabla \mathrm{g} \\ \nabla \mathrm{h}^{\mathrm{T}} & 0 & 0 \\ \nabla g^{\mathrm{T}} & 0 & 0 \end{bmatrix}^{-1}}_{\nabla^2 \mathcal{L}} \underbrace{\begin{bmatrix} \nabla \mathrm{f} + \lambda_k \nabla \mathrm{h} + \sigma_k \nabla \mathrm{g} \\ h \\ g \end{bmatrix}}_{\nabla \mathcal{L}}$$
$$\begin{bmatrix} x_{k+1} \\ \lambda_{k+1} \\ \sigma_{k+1} \end{bmatrix} = \begin{bmatrix} x_k \\ \lambda_k \\ \sigma_k \end{bmatrix} - \left(\nabla^2 L\right)^{-1} \nabla \mathrm{L} \tag{4}$$

Nevertheless, the $\nabla^2 L$ matrix is frequently a singular or ill-conditioned matrix, so the Newton step term ($d\ d = \left(\nabla^2 L\right)^{-1} \nabla \mathrm{L}$) cannot be calculated directly. Instead, the basic sequential quadratic programming algorithm (SQP algorithm) defines an appropriate search direction "*d*" as an iteration process to solve the Newton step. The sequential quadratic problem is applied as follows:

$$\begin{array}{cc} Min_d & f(x_k) + \nabla f(x_k)^T d + \frac{1}{2} d \nabla^2_{xx} L(x_k,\ \lambda_k, \sigma_k) d \\ Regarding & h(x_k) + \nabla \mathrm{h}(\mathrm{x_k})^{\mathrm{T}} \mathrm{d} \geq 0 \\ & g(x_k) + \nabla \mathrm{g}(\mathrm{x_k})^{\mathrm{T}} d = 0 \end{array} \tag{5}$$

Once the Newton step term is found, the process is repeated by a number "i" of iterations until convergence is reached; see Figure 5. The main reason to choose this method

is solving an equation system with non-linear constraints, which is a robust method with a fast convergence rate in comparison to other methods such as de Nelder–Mead or Powell.

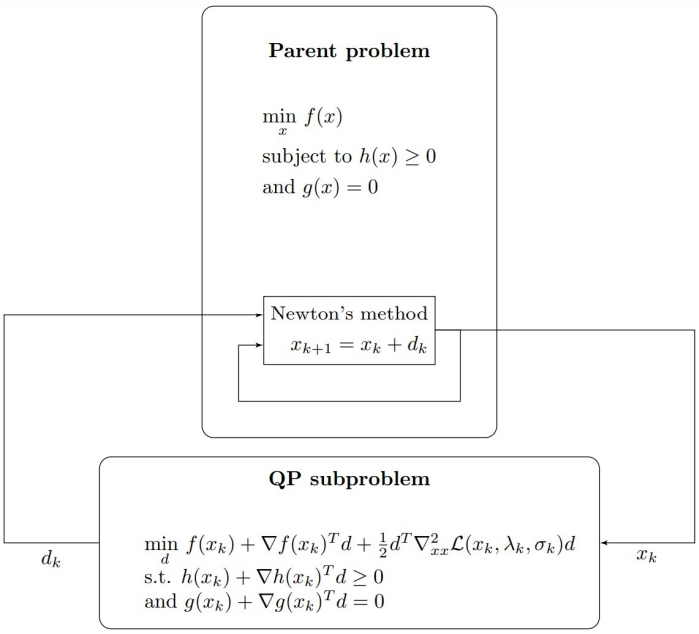


Figure 5. Scheme of SLSQP method.

2.2. The OPF Algorithm

The OPF algorithm solves the mass and energy balance equation at irrigation canals and regulation reservoirs regarding water levels and crop water demands. On the other hand, the algorithm also considers the hydraulic power and energy expense equations related to the pumping station and energy price market, respectively.

A summary of the OPF algorithm schedule is the following. The algorithm solves a constrained optimization problem where the unknown variable is the pumping flow trajectory, where the objective function is the energy expense during the irrigation cycle, the inequality constraints refer to the maximum and minimum water levels of the reservoir as well as the maximum pumping flow, and the equality constraint makes reference to the mass and energy balance equation.

2.2.1. Objective Function: Energy Expenses Equation

The hydraulic power equation for a pumping station is the following:

$$\begin{aligned} P_t(t) &= \rho g\left(Q_{pumping}(t) Hb_k(t)\right) \\ E_{expenses}(t) &= P_t(t) \Delta t E_{price}(t) \end{aligned} \tag{6}$$

where ρ is the water density, g is the gravity term, Δt is the time step, $Q_{\ pumping}(t)$ is the pumping flow trajectory from the canal to the reservoir, i.e., a vector with x elements (x being the number of pump flow operations during a horizon time of period), and $Hb_k(t)$ is the pump head trajectory among the irrigation canal section and the reservoir, i.e., a vector with x elements as well; see Figure 4.

On the other hand, $E_{expenses}(t)$ is the energy expenses trajectory during the horizon time period and E_{price} is the energy price trajectory during the horizon time period, both vectors with an x element. In that sense, the optimal solution is obtained by minimizing the performance criterium, where $E_{minimum}(t)$ is the minimum energy expense trajectory (i.e., non-energy cost).

$$Minimize\ J(E) = minimize\left(\frac{1}{2}\left[E_{expenses}(t) - E_{minimum}(t)\right]^T \left[E_{expenses}(t) - E_{minimum}(t)\right]\right) \tag{7}$$

We have to mention that pump characteristics curves have not been considered in the OPF algorithm in order to reduce the complexity of the system. In that sense, the pumping station efficiency value is considered as 1.

Every pump flow operation period is equal to the energy price discretization, i.e., 1 h, and we consider incompressible flow.

Regarding pumping flow trajectories, pump head trajectory and energy price can be approached by piecewise functions, so these functions are also defined by vectors considering a constant value for every time step (Δt).

2.2.2. Inequality Constraints

The inequality constraints applied in the equation system are the following:

Reservoir Condition

The reservoir water level must be located among a water level range of values due to maintenance and operation constraints; see Figure 6.

$$H_{min} < H(t) < H_{max} \tag{8}$$

where H is the water level at the regulatory reservoirs, T_a is the width of the wall of a reservoir, and H_{max} and H_{min} are the maximum and minimum water levels at the reservoir, respectively.

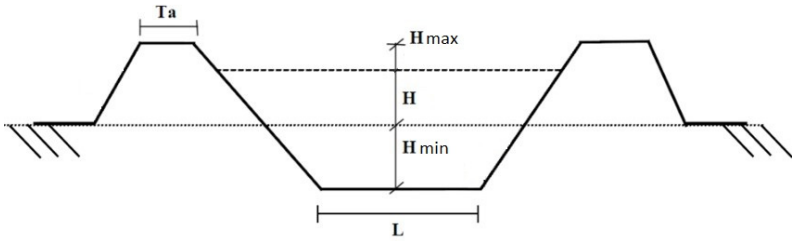


Figure 6. Inequality constraints regarding reservoir conditions.

Pumping Station Condition

The pipeline, which connects the irrigation canal and regulatory reservoir (see Figure 7), is working regarding a maximum water flow in order to keep the pipe wall integrity.

$$Q_{k\text{pumping}}(t) < Q_{max} \tag{9}$$

where Q_{max} is the pipeline's maximum flow allowed according to canal geometry and conditions (water level) as well as the pipeline size and velocity requirements.

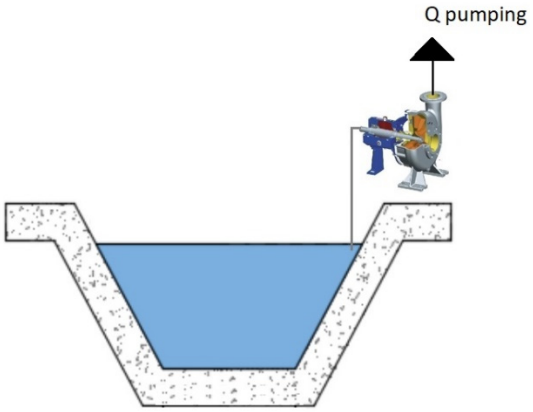


Figure 7. Inequality constraints regarding pumping station conditions.

2.2.3. Boundary Conditions

In that sense, the crop water demand was estimated from the type of crop and reference evapotranspiration value considering the Penman–Monteith formulation, the most accurate formulation according to the FAO (Smith et al. [26]).

$$ET_c(t) = ET_0(t)K_c(t) \tag{10}$$

where $ET_c(t)$ is the total crop evapotranspiration (mm/h) per tree and period of year, ET_0 (t) is the reference evapotranspiration (mm/h) per tree depending on the temperature calculated from the Penman–Monteith formulation and period of year, and $K_c(t)$ is a dimensionless parameter depending on the type of crop and period of the year.

The reference evapotranspiration formulation is out of the scope of this manuscript (see Smith et al. [26]), and its values have been estimated considering weather conditions every hour for a week.

2.2.4. Equality Constraints

Mass Balance Equation

Regarding the mass balance equation at the reservoir, there are several elements to consider: reservoir water volume, crop water demand ($Q_{\text{reservoir outlet gravity}}$, see Figure 4) and pumping flow (Q_{pumping}; see Figure 4), as follows:

$$\begin{gathered} \Delta M(t) = \rho \left(\sum_{k=0}^{mp} Q_{k\ (pumping)}(t)\Delta t - \sum_{j=}^{mc} Q_{j\ (crops\ demand)}(t)\Delta t \right) \\ \rho \times \left(Q_{k\ (pumping)}(t)\Delta t - Q_{j\ (crops\ demand)}(t)\Delta t \right) - \Delta M(t) = 0 \end{gathered} \tag{11}$$

where ΔM is the reservoir mass variation between time steps, i.e., a vector with x elements (with the same size of pumping flow trajectory), mp is the number of pump stations, j is the number of crops associated with the regulatory reservoir, Δt is the time step, $Q_{j(crops\ demands)}(t)$ is the flow demand trajectory for crop "j", i.e., a vector with x elements (with the same size of pumping flow trajectory) and mc is the number of type of crops.

Crop flow demand trajectories and pumping flow trajectories can be approached with piecewise functions, so both functions are also defined by vectors considering a constant value for every time step (Δt).

Energy Balance Equation

The energy balance equation (Bernoulli equation) developed for fully rough–turbulent pipe flow from the irrigation canal to the regulatory reservoir is formulated as follows:

$$\begin{gathered} z_l + \frac{P_l}{\gamma} + \frac{v_l^2}{2g} + Hb_k = z_i + \frac{P_i}{\gamma} + \frac{v_i^2}{2g} + \Delta H_R \\ z_l + \frac{P_l}{\gamma} + \frac{v_l^2}{2g} + Hb_k - \left(z_i + \frac{P_i}{\gamma} + \frac{v_i^2}{2g} + \Delta H_R \right) = 0 \end{gathered} \tag{12}$$

where l represents an irrigation canal section and i represents a regulatory reservoir, z_i and z_l are the height of sections "i" and "l", respectively, P_i and P_l are the pressure of sections "i" and "l", respectively, Hb is the pumping head, v_i or v_l are the water velocities of sections "i" and "l", respectively, and ΔH_R is the energy loss between both sections ("i" and "l"), which is defined as follows:

$$\Delta H_R = f \frac{L}{\varnothing} \frac{v^2}{2g} \tag{13}$$

where f is the Darcy Weisbach parameter, L is the pipe length between sections ("l" and "i"), v is the water velocity through piping between sections ("l" and "i") and $\varnothing$ is the

pipe diameter. In order to reduce calculation complexity, the Darcy Weisbach parameter is estimated previously as a constant value considering fully rough turbulent flow.

2.3. GoRoSo Algorithm

The GoRoSo algorithm is an essential part of the overall control diagram; see Figure 3. GoRoSo calculates the optimum gate trajectories for the irrigation canal for a horizon time period, regarding the initial irrigation canal conditions, pumping flow trajectories and water demand at the gravity orifice offtake. In that sense, the water demand is estimated previously from the reference water levels at target points, which are located at the bottom of particular cross-sections along the canal (Figure 4). The GoRoSo algorithm estimates the optimum gate trajectory for all gates in the irrigation canal over an irrigation cycle and evaluates the error between the desired water level at target points and the real water level at those points. The residual error must be lower than a specific value (for all irrigation cycles) to solve the optimization problem and stop the iterative process. Once the optimum gate trajectories are estimated, the canal water levels are also known in every cross-section along the canal for the horizon time period, so the water levels close to the pumping stations are also known.

All this information is shared with the OPF algorithm, which calculates the optimum pumping trajectories according to the regulatory reservoir and irrigation canal requirements, providing crop water demands (located upstream from the irrigation canal) and minimizing the pumping energy expenses. As we mentioned before, the GoRoSo algorithm is out of the scope of this work as this algorithm has been published in several journals previously; see Soler et al. [11].

3. Results and Discussion

Two test cases are tested in this section in order to check the OPF algorithm capabilities. First of all, OPF is tested alone, i.e., the algorithm is tested without the GoRoSo algorithm, so the irrigation canal conditions are irrelevant for this test and the OPF algorithm assumes the water level at the irrigation canal sections remains constant during this scenario. In a second test, the OPF algorithm is tested with the GoRoSo algorithm, so the irrigation canal conditions, such as unsteady water level or flow, are unsteady during the horizon time period.

3.1. Scenario I: Pumping Flow Optimization Considering Two Regulation Reservoirs and Stationary Water Level at the Irrigation Canal

In this numerical example, the OPF algorithm is tested assuming two regulation reservoirs that have no hydraulic influence on each other, because we assume in this scenario that the water level is steady at the pumping station location; see Figure 8. In that sense, pumping flow trajectories do not affect downstream and upstream flow conditions at the irrigation canal.

3.1.1. System Features

The system features are as follows in Tables 1 and 2:

Table 1. Regulatory reservoir features in scenario I.

Regulatory Reservoir Number	Square Regulatory Reservoir Bottom (Width and Length) (m)	Reservoir Wall Slope (H:V)	Reservoir Depth (m)
I	35	1/3:1	2
II	35	1/3:1	2

On the other hand, the cast iron pipeline features are introduced in the following table:

Table 2. Pipelines features in scenario I.

Pipeline (Connected with Regulatory Reservoir Number)	Length (m)	Diameter (mm)	Absolute Pipe Roughness (mm)
1	2000	90	0.5
2	2000	90	0.5

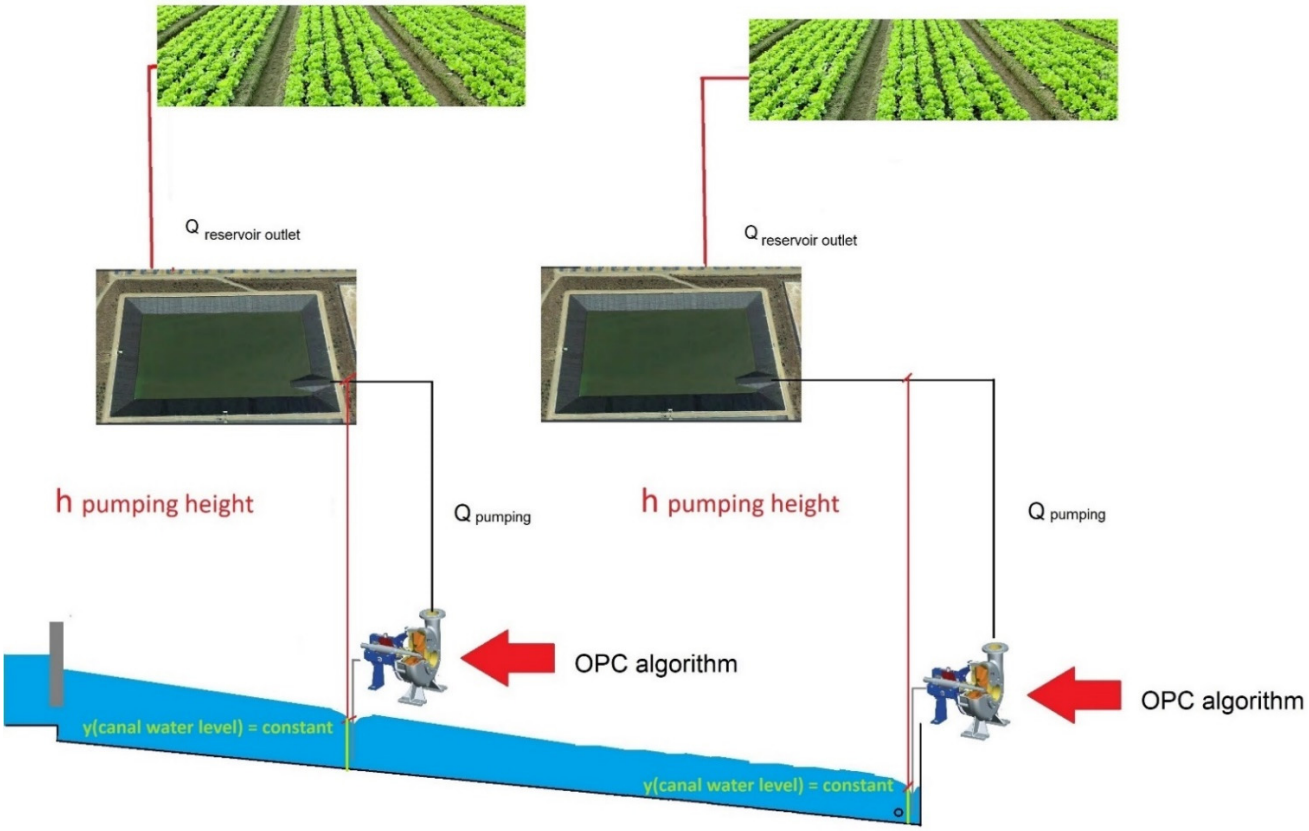


Figure 8. The system features in scenario I.

3.1.2. Boundary Conditions

The crop water demand associated with regulatory reservoir n°1 (i.e., cherry crops) and n°2 (i.e., peach crops) is introduced in Figures 9 and 10, regarding the evapotranspiration formulation (9) using a Kc value for both crops equal to 0.9 and considering 4000 cherry trees (see Figure 9) and 5000 peach trees (see Figure 10). Regarding the reference evapotranspiration value (mm/h), it was estimated from the Penman–Monteith formulation regarding hourly weather conditions from 20 June 2020 to 26 June 2020 at Lleida (Spain).

On the other hand, the horizon period of time is 4 weeks for this scenario and the weather conditions for 1 week (20 June 2020 to 26 June 2020) were reproduced equally during the next 3 weeks, so the weather conditions are the same every week during the four weeks.

On the other hand, the time step between successive control actions (pump station operations) is determined to be equal to T = 1 h. This regulation period was established due to the energy price and crop flow demand requirements, and both datasets were discretized using an hourly time period established by the electricity market operator and the Spanish State Meteorological Agency, respectively. In this sense, the crop flow demand and pump flow trajectories are defined by vectors with 672 elements (24 h × 7 days × 4 weeks).

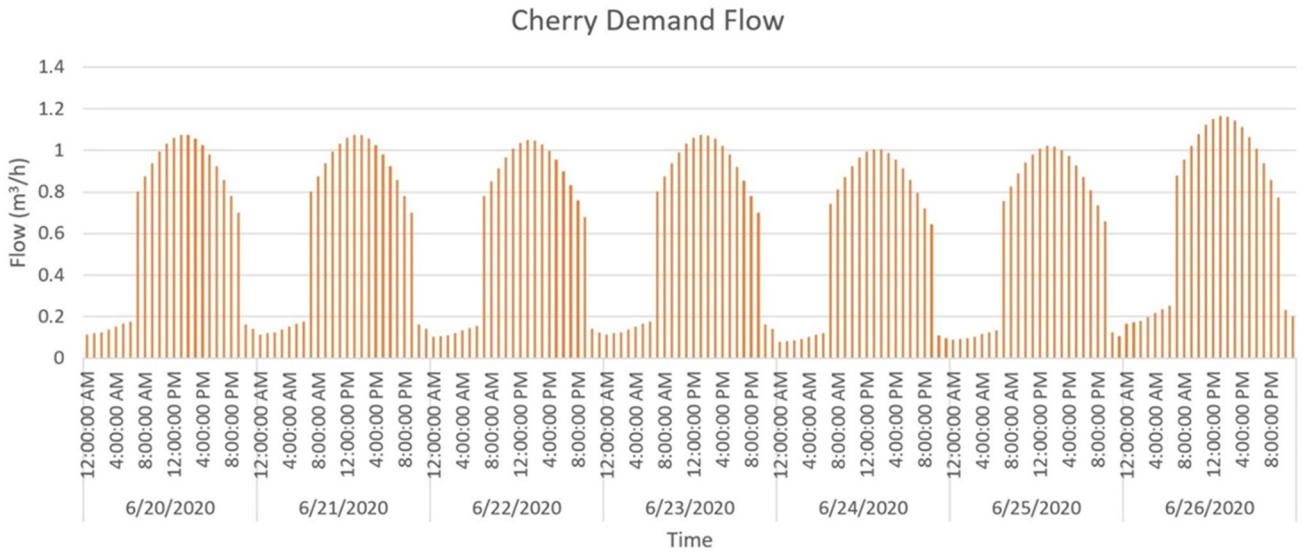


Figure 9. The cherry demand flow associated with regulatory reservoir n°2 for a week (20 June 2020 to 26 June 2020).

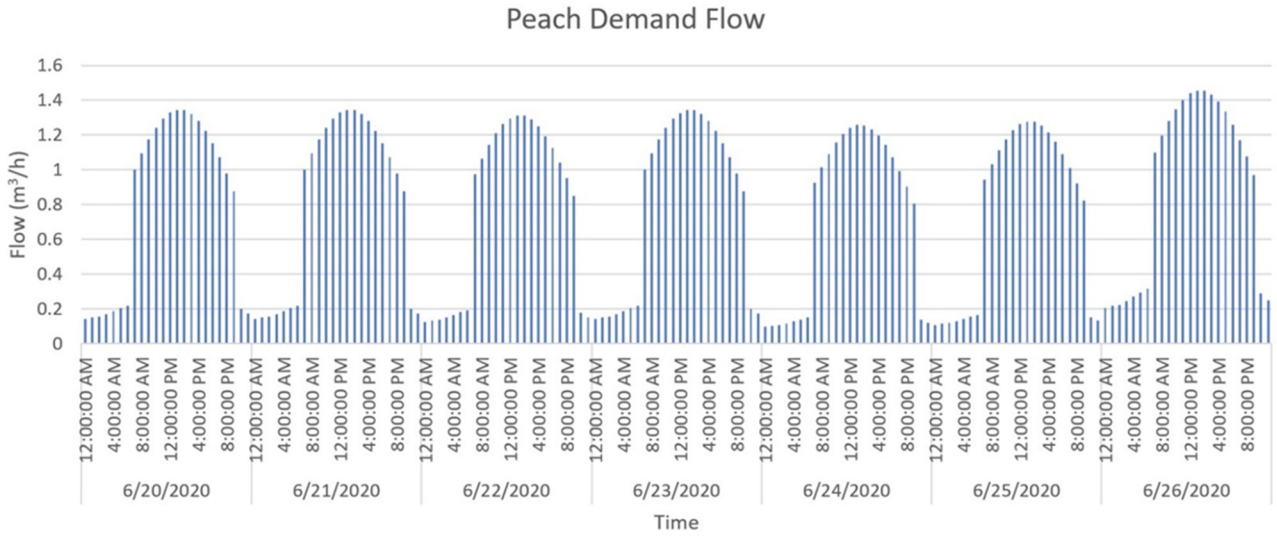


Figure 10. The peach demand flow associated with regulatory reservoir n°1 for a week (20 June 2020 to 26 June 2020).

3.1.3. Initial Conditions

The initial conditions for this scenario are shown in Table 3.

Table 3. Initial conditions in scenario I.

Regulatory Reservoir Number	$H_{reservoir}$ (Height between Bottom and Water Level at Regulatory Reservoir)(m)	H_{total} (Total Height between Irrigation Canal Bottom and Regulatory Reservoir Water Level) (m)	Y (Canal Water Level at Pump Station Location) (m)	$h_{pumping\ height}$ (H_{total}-Y) (m)
1	1.5	316 m.c.a.	2 m.c.a.	314 m.c.a.
2	1.5	316 m.c.a.	2 m.c.a.	314 m.c.a.

3.1.4. Constraint Conditions

The inequality constraints conditions adopted in this test according to regulatory reservoir and pipeline requirements are the following:

$$\begin{gathered} 1 \text{ m.c.a.} < H_i(t) < 1.8 \text{ m.c.a} \\ Q_{k\text{pumping}}(t) < 25 \ \tfrac{\text{m}^3}{\text{h}} \end{gathered} \tag{14}$$

3.1.5. Energy Price

The energy price is provided by REE (Red Eléctrica de España) using an hourly time period considering the PVPC (Voluntary Price for the Small Consumer) methodology. A simple example, for just a day, is shown in Table 4; as you can see, the price is increasing during the peak production hours and decreasing during the off-peak hours.

Table 4. Energy price provided by REE in KW/h.

Time	Price (kW/h)	Time	Price (kW/h)	Time	Price (kW/h)	Time	Price (kW/h)
00:00	0.11633	07:00	0.1157	14:00	0.13796	21:00	0.24808
01:00	0.11595	08:00	0.15289	15:00	0.13288	22:00	0.15591
02:00	0.11489	09:00	0.15083	16:00	0.13193	23:00	0.1565
03:00	0.11496	10:00	0.24262	17:00	0.13599	24:00	0.11633
04:00	0.11484	11:00	0.2405	18:00	0.23144		
05:00	0.11603	12:00	0.23809	19:00	0.2404		
06:00	0.11629	13:00	0.2353	20:00	0.2462		

3.1.6. Results

As you can see in Figure 11, the OPF algorithm calculates an optimum solution (pumping flow trajectories) regarding cumulative energy expenses, as both pumping stations are consuming energy just in case the energy price is cheaper, i.e., during the weekend, and the accumulative energy expenses keep steady during the week, because the energy at peak hours is more expensive.

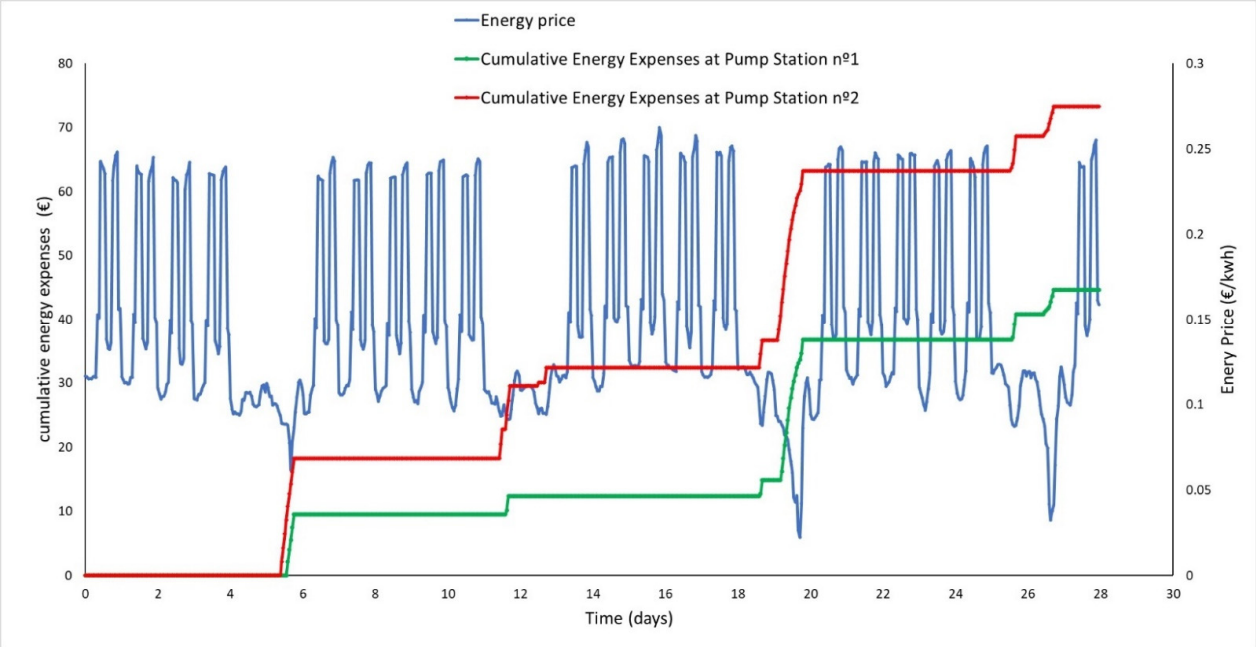


Figure 11. The energy price vs. cumulative energy expenses at pump stations n°1 and n°2 in scenario I.

On the other hand, we can see in Figure 12 that reservoir n°2 has larger water level fluctuations than reservoir n°1, which is associated with a greater crop water demand (peach crops) and frequent operation of pumping station n°2. The OPF algorithm calculates an optimum solution considering that the water level at the reservoir cannot be lower than 1 m.c.a. or greater than 1.8 m.c.a., and pumping flow is never greater than 25 m^3/h, optimizing energy expenses; see Figure 12. On the other hand, pump stations do not always need to operate during off-peak time periods; this depends on the water level in the reservoir and the crop flow demands throughout the time horizon. As you can see, the pumping stations are not operating during the first days of the horizon time period, because the water level at regulatory reservoirs is close to 1.5 m.c.a.; once the water level at regulatory reservoirs is lower, the pumping stations start to work, but in any case, the pumping stations only operate during off-peak hours, because this is the optimum option for scenario I.

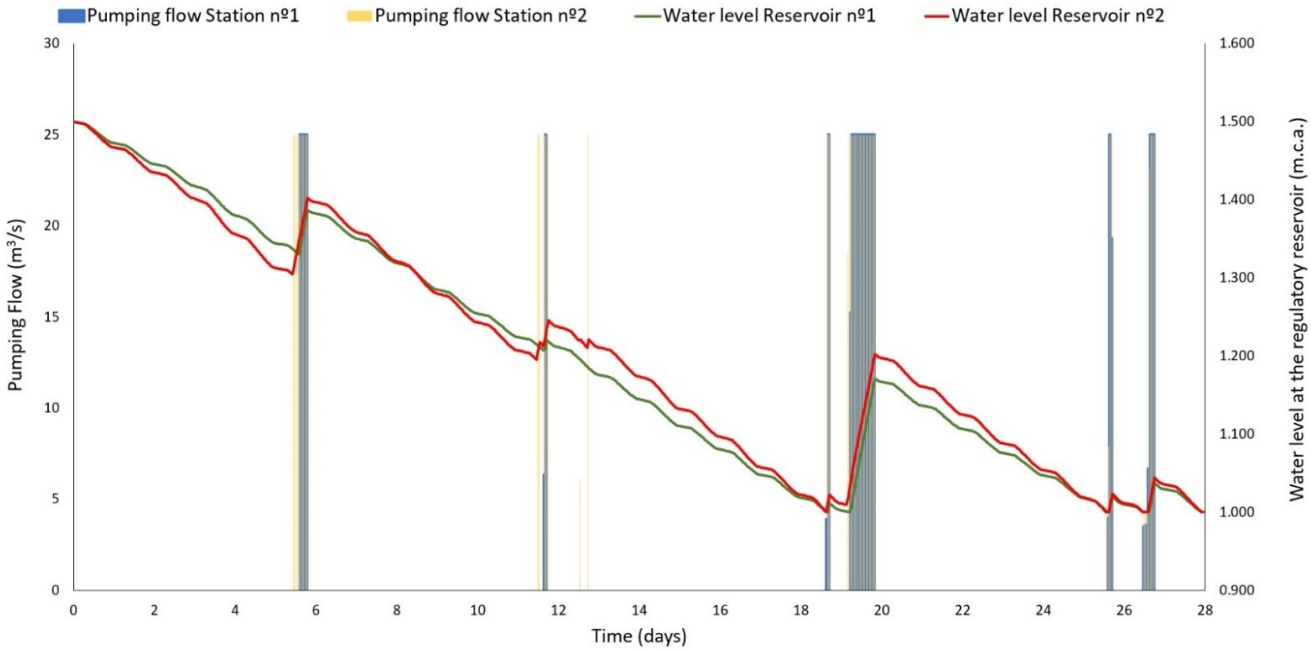


Figure 12. Pumping flow at stations n°1 and n°2 (column chart) vs. water level at regulatory reservoirs n°1 and n°2 (line chart) in scenario I.

The OPF algorithm worked properly for scenario I, so the algorithm was tested in a much more demanding scenario II.

3.2. Scenario II: Pumping Flow Optimization Considering Two Regulation Reservoirs and Non-stationary Water Level at the Irrigation Canal Based on the ASCE Test Case

This scenario is developed according to the overall control diagram (offline computation). First of all, GoRoSo calculates the optimum gate trajectories regarding scheduled water demands, i.e., gravity orifice offtake for the complete irrigation cycle and initial pumping flow trajectories. All this information is shared with the OPF algorithm which calculates again the optimum pumping flow trajectories regarding regulatory reservoir condition, crop water demand, irrigation canal condition and as energy expenses.

As we mentioned before, all these processes are running in an iterative way, so GoRoSo and OPF recalculate the optimum gates and pumping flow trajectories once again until convergence is reached. The iterative process stops when the residual error is minimized and there are no changes in the gate and pumping flow trajectories, reaching an optimal solution. The processes template of the overall control diagram is introduced in Figure 5.

In this scenario II, the OPF algorithm is also tested assuming two regulation reservoirs are connected to a pumping station, but the irrigation canals's behaviour is also considered.

In that sense, both pumping stations introduce water level and flow perturbations at the irrigation canal just in case pumping stations are operating. Therefore, pumping stations can influence the flow conditions in the canal. In conclusion, the OPF algorithm operates alongside the GoRoSo algorithm, as both algorithms calculate pumping flow trajectories and canal gates trajectories, respectively, in an iterative process.

For this scenario, we introduce the test cases that were proposed by the ASCE committee to evaluate control algorithms (Clemmens et al. [13]), so irrigation canal features for the GoRoSo algorithm are provided by test case 22. On the other hand, the OPF algorithm considers the same initial and boundary conditions and equality constraints as described in scenario I. Instead, the pipeline inequality constraint was adapted to the new scenario II, with a maximum pumping flow of 1 m^3/s, because boundary conditions were estimated considering a higher crop flow demand than scenario I.

3.2.1. Irrigation Canal

The ASCE committee's proposed test cases (Clemmens et al. [13]) are evaluated using the Corning Canal, which is based on the upstream portion of the actual Corning Canal in California. This canal is characterized by its length, gentle slope, and significant storage capacity. Spanning 28 km, the canal features trapezoidal cross-sections and is divided into eight pools separated by rectangular gates. The canal is delimited by a total of nine points (numbered 0 to 8), as illustrated in Figure 13. The first point (0) solely contains the initial sluice gate, serving as a boundary between the canal and a large reservoir; it is not considered a checkpoint. Additional hydraulic structures along the canal include orifice offtakes, emergency lateral spillways, and pump stations, all located at the downstream end of each pool, where water level measurements are taken.

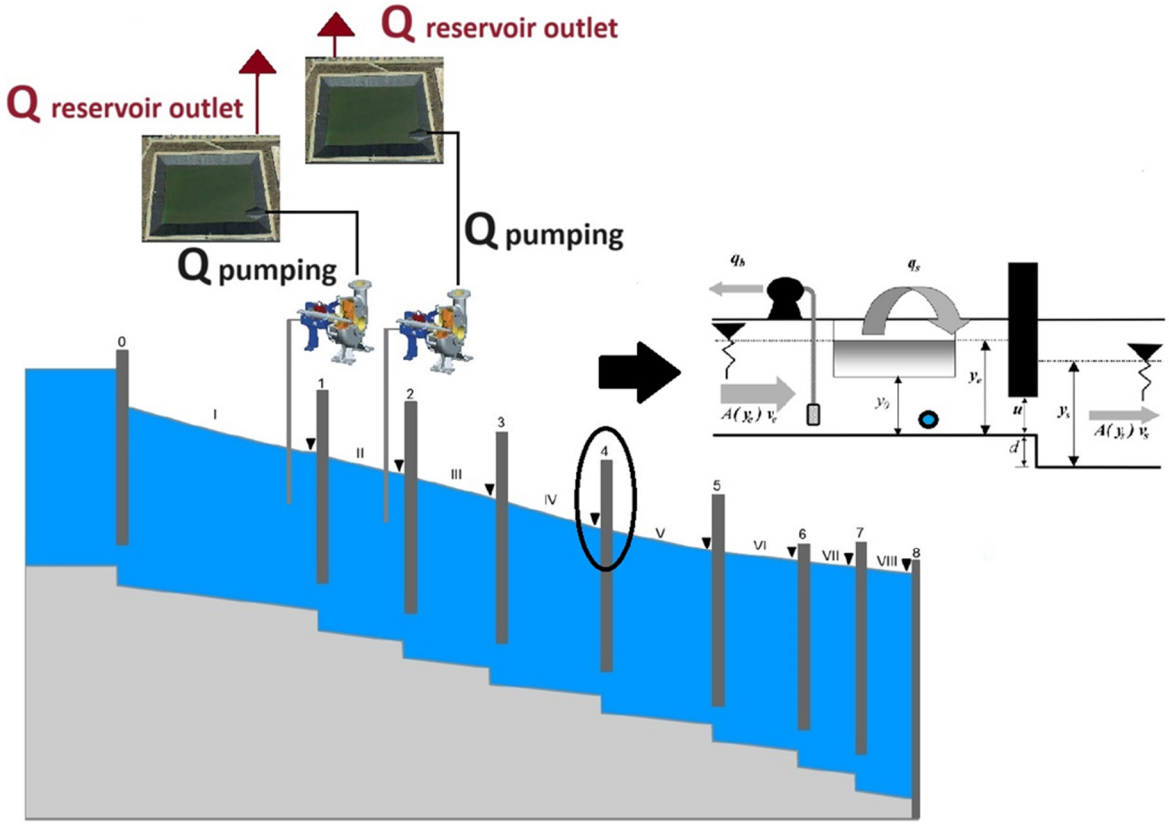


Figure 13. Corning Canal profile. The triangles mark the position of checkpoints (which are defined by a pump station, gravity orifice offtake, lateral discharge, gate and water level sensor; see the figure on the right). The first pool is number I and the first checkpoint is number 1.

Figure 13 illustrates the geometry of the canal, including the numbering scheme for the pools and nodes utilized. Table 5 provides an overview of the general characteristics of the canal pools, while Table 6 outlines the features of the hydraulic control structures at each node. Additionally, Table 6 includes the pump station number corresponding to a specific target point.

Table 5. Features of Corning Canal pools.

Pool Number	Pool Length (km)	Bottom Slope	Side Slopes (H:V)	Manning's Coefficient (n)	Bottom Width (m)	Canal Depth (m)
I	7	10×10^{-4}	1.5:1	0.02	7	2.5
II	3	10×10^{-4}	1.5:1	0.02	7	2.5
III	3	10×10^{-4}	1.5:1	0.02	7	2.5
IV	4	10×10^{-4}	1.5:1	0.02	6	2.3
V	4	10×10^{-4}	1.5:1	0.02	6	2.3
VI	3	10×10^{-4}	1.5:1	0.02	5	2.3
VII	2	10×10^{-4}	1.5:1	0.02	5	1.9
VIII	2	10×10^{-4}	1.5:1	0.02	5	1.9

Table 6. Corning Canal control structures (0* the pumping station only pumps the excess flow from the last pool of the canal).

Target Points	Gate Discharge Coefficient	Gate Width (m)	Gate Height (m)	Step (m)	Length from Gate 1 (km)	Orifice Offtake Height (m)	Lateral Spillway Height (m)	Pump Station Number
0	0.61	7	2.3	0.2	0	-	3	-
1	0.61	7	2.3	0.2	7	1.05	2.5	1
2	0.61	7	2.3	0.2	10	1.05	2.5	2
3	0.61	7	2.3	0.2	13	1.05	2.5	-
4	0.61	6	2.1	0.2	17	0.95	2.3	-
5	0.61	6	2.1	0.2	21	0.95	2.3	-
6	0.61	5	1.8	0.2	24	0.85	1.9	-
7	0.61	5	1.8	0.2	26	0.85	1.9	-
8	-	-	-	-	28	0.85	1.9	0*

As previously mentioned, the test case presented in this paper is based on test case 2-2. The simulation's time horizon is set at 12 h (43,200 s). The time interval between successive control actions for canal gates is established at T = 900 s (15 min). However, for pumping flow actions, the time interval between successive control actions is set at T = 3600 s (1 h). Thus, canal gates can operate four times faster than pumping stations.

The upper boundary condition is set by a constant water level provided by a large reservoir upstream from the first gate at the Corning Canal, which is equal to 3 m over the entire simulation. Conversely, the boundary conditions for each pool are determined by the discharge through the gravity orifice offtake and the flow extracted by the pump, both located downstream of each pool.

At the end of the canal, the pump extracts a constant water flow of 3 m^3/s. The initial conditions for the test case, detailed in Table 7, correspond to the initial steady state of the canal, as well as the gravity flow demand at the orifice offtake. It be should noted that

pump stations are not operating at initial conditions, so the flow perturbations introduced into the canal when pump stations start to operate are significant.

Table 7. Corning Canal initial and boundary conditions.

Pool Number	Gravity Orifice Offtake Flow (m^3/s)	Check Initial Flow (m^3/s)	Target Water Level (m)	Pumping Flow (m^3/s)
Heading	-	13.5	-	0
I	1.0	12.5	2.1	0
II	1.0	11.5	2.1	0
III	1.0	10.5	2.1	0
IV	1.0	9.5	1.9	0
V	2.5	7.0	1.9	0
VI	2.0	5.0	1.7	0
VII	1.0	4.0	1.7	0
VIII	1.0	3.0	1.7	3

Furthermore, the canal is required to maintain certain values of water levels at the checkpoints as it controls the flows through the gravity orifice offtakes, and the watermaster must deliver the scheduled delivery demands downstream of the canal during the whole irrigation cycle, which, in this test case, lasts 12 h. The desired water levels or target levels are introduced in Table 7 for each checkpoint in the Corning Canal, which is also the location to measure the water level at every time step (every 900 s).

3.2.2. Reservoir and Pipeline System

On the other hand, the reservoir features and initial conditions, as well as pipeline features, are represented in Tables 8–10.

Table 8. Regulatory reservoir features.

Regulatory Reservoir Number	Square Reservoir Bottom (Width and Length) (m)	Reservoir Wall Slope (H:V)	Reservoir Depth (m)
1	303	1/3:1	2
2	311	1/3:1	2

Table 9. Regulatory reservoirs and system initial conditions.

Regulatory Reservoir Number	Initial $H_{reservoir}$ (Height among Bottom and Water Level at Regulatory Reservoir (m.c.a.)	H_{total} (Total Height among Irrigation Canal Bottom and Regulatory Reservoir Water Level) (m.c.a.)	*Y (Water Level at Canal Section) (m.c.a.)	h Pumping Height (H_{total}-Y) (m.c.a.)
1	1.5	38 m.c.a.	2 m.c.a.	36 m.c.a.
2	1.5	38 m.c.a.	2 m.c.a.	36 m.c.a.

*Y: water level at a particular canal section which matches with pump stations.

Table 10. Pipeline features.

Pipeline (Connected with Regulatory Reservoir Number)	Length (m)	Diameter (mm)	Absolute Pipe Roughness (mm)
1	1100	800	0.5
2	1100	800	0.5

3.2.3. Constraint Conditions

The inequality constraint conditions adopted in this test are the following:

$$\begin{array}{c} 1 \text{ m.c.a.} < H_i(t) < 1.8 \text{ m.c.a} \\ Q_{k\text{pumping}}(t) < 1 \ \frac{\text{m}3}{\text{s}} \end{array} \quad (15)$$

3.2.4. Crop Flow Demand

The crop flow demand is based on flow demand in scenario I, although the number of trees in this scenario has increased by a lot because there are 5000 ha of cherry trees and 6250 ha of peach trees (considering 2880 trees per ha); see Figure 14. The crop flow demand has been estimated taking into account the irrigation canal conditions as well as the horizon time period (12 h).

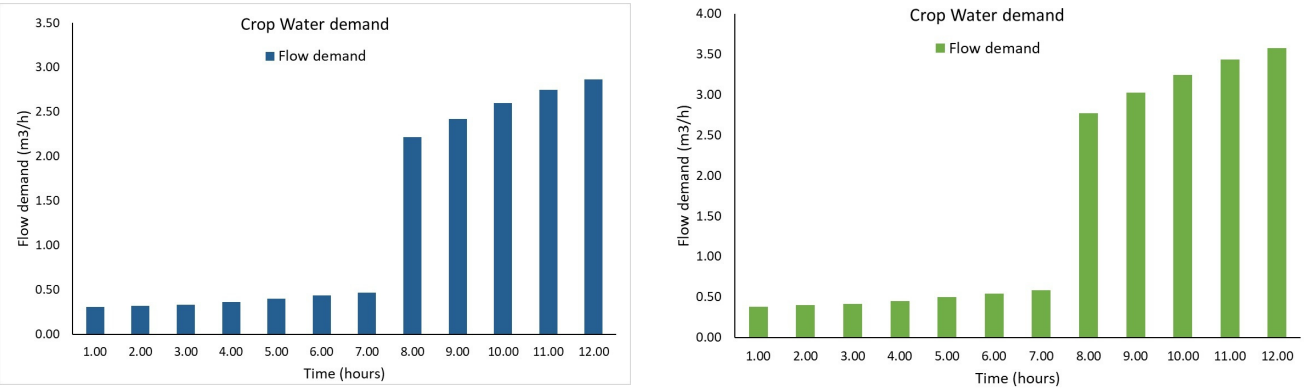


Figure 14. The crop water demands associated with regulatory reservoirs 1 (**left**) and 2 (**right**), i.e., cherry crops and peach crops, respectively.

3.2.5. Energy Prices

The energy price is similar to that in Table 4 proposed for scenario II, although the energy price for several time steps has been increased; the second, third and ninth hours have been increased five times in order to check the adaptability of the OPF algorithm in case of big changes in electricity tariffs.

3.2.6. Results

As you can see in Figure 15, the OPF algorithm optimizes the pumping flow trajectories, because both pumping stations are consuming energy just in case the energy price is cheaper, e.g., between the fourth and eighth hour.

On the other hand, we can see from Figure 16 that reservoir n°2, which is related to a greater crop water demand, has larger water level fluctuations than reservoir n°1 during the time horizon. In this sense, pumping station n°2 is also operating when the water reservoir is full of water (4–8 h), increasing the water level to 1.6 m.c.a. (from 1.5 m.c.a. to 1.6 m.c.a.) when the energy price is cheaper. The algorithm is looking to increase the water volume of reservoir n°2 because crop flow demand is going to increase in the future, when the energy price will be more expensive.

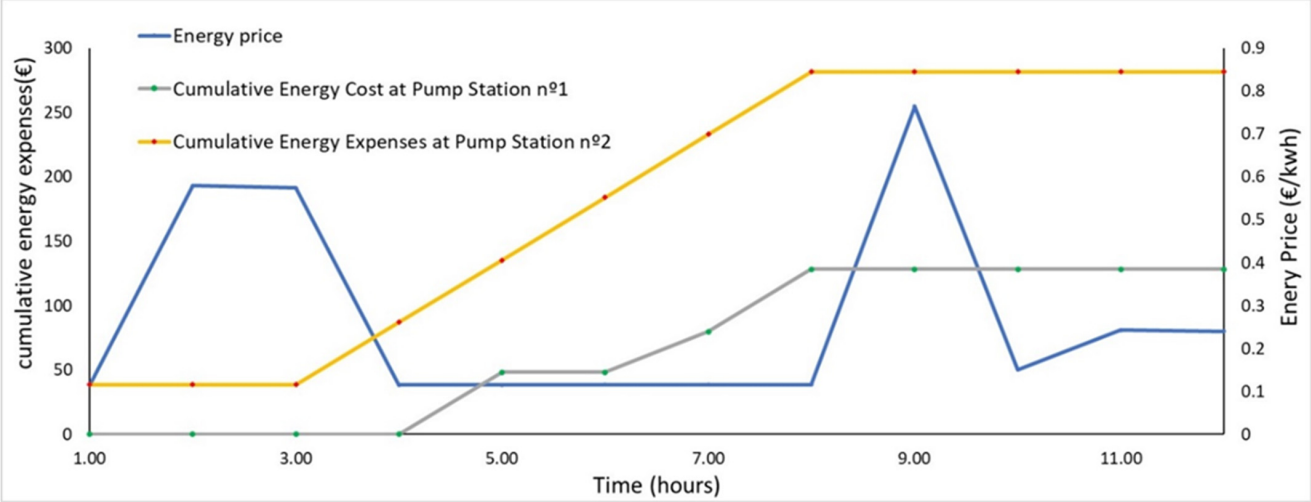


Figure 15. The energy price vs. cumulative energy expenses at pump stations n°1 and n°2 in scenario II.

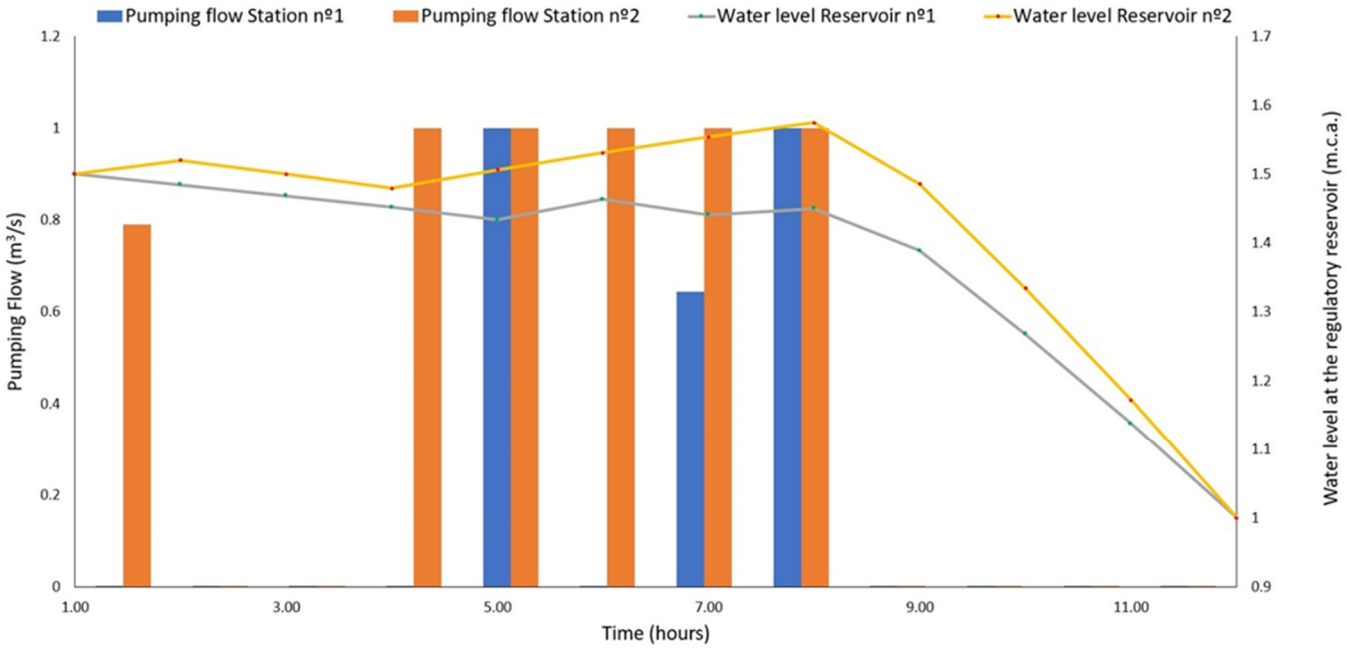


Figure 16. Pumping flow at stations n°1 and n°2 vs. water level at regulatory reservoirs n°1 and n°2 in scenario II.

On the other hand, the OPF algorithm calculates an optimum solution considering that the water level of the reservoir cannot be below 1 m.c.a. (inequality constraint). But in any case, the pumping flow is never greater than 1 m^3/s, which is the other inequality constraint. On the other hand, the reservoir water level will be recovered to the initial water level (1.5 m.c.a.) over the next 12 h at night, when the energy price is also cheap.

Regarding the GoRoSo algorithm, canal gate trajectories have been recalculated considering new pumping flow trajectories, for instance, when pump station n°2 is pumping its flow at the first hour, gate n°0 (upstream of pumping station n°2) is opening to increase the flow into the irrigation canal (the gate reference position is 0.3 in the case where the pump stations are not operating and 0.475 in the case where the pump stations are operating during the first hour; see Figure 17), because the water level at target point n°2 (in the same location as pump station n°2; see Figure 13) is decreasing; see Figure 18. On the other side, gate n°2 closes at the first hour in order to reduce the downstream flow, because gate n°2 is in the same location as pump station n°2 and target point 2; see Figures 13 and 17. In

this sense, gate n°2 reduces the downstream flow at the first hour, in order to keep the water level at target point 2 (and supply the water demand at the gravity orifice's offtake), which is also decreasing due to pump station n°2. Once extra flow from gate n°0 arrives at target point 2, after the first hour, gate n°2 starts to open because the water levels at the downstream target points (3,4,5,6,7) are also decreasing, and GoRoSo wants to recover them as soon as possible. In the end, taking into account that pumping stations are not operative from the ninth to twelfth hour, all gates recover their initial positions in order to keep the water level at canal target points just considering the water demand at the gravity orifice's offtake. On the other hand, water levels are measured by sensors at target points. The accuracy of these measurements may vary depending on the sensor used, which could potentially impact the accuracy of the GoRoSo algorithm. Additionally, sensitivity analysis was performed to address errors in water level measurements by the sensor. However, this analysis is beyond the scope of this manuscript but can be referenced in Bonet, E. 2015 [27].

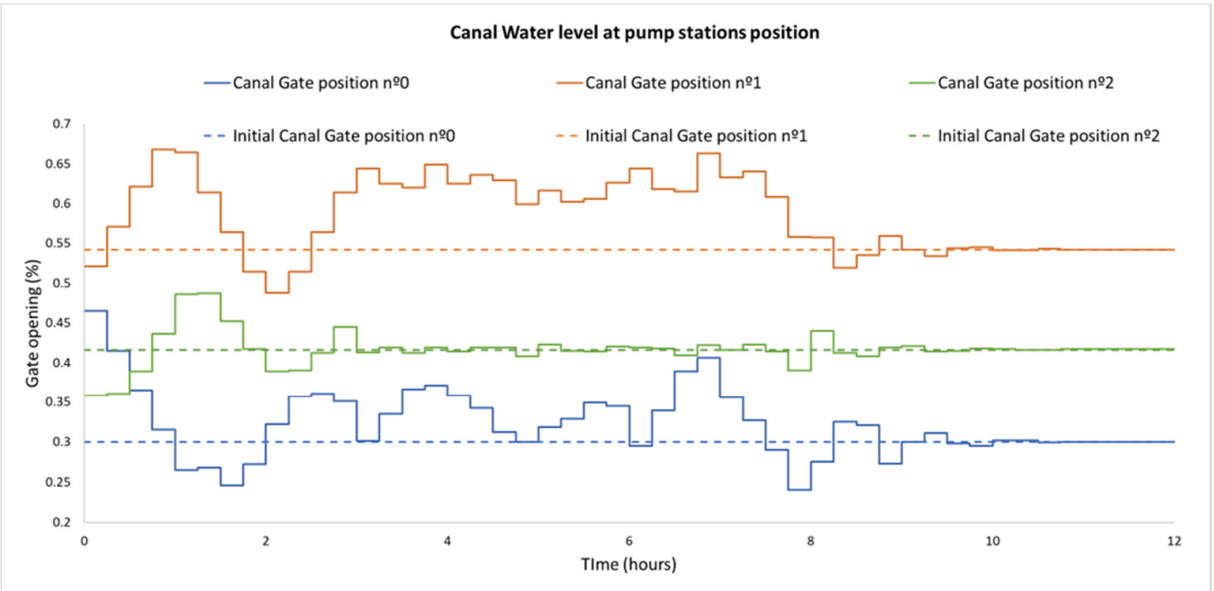


Figure 17. Gates n°0, 1 and 2 in scenario II.

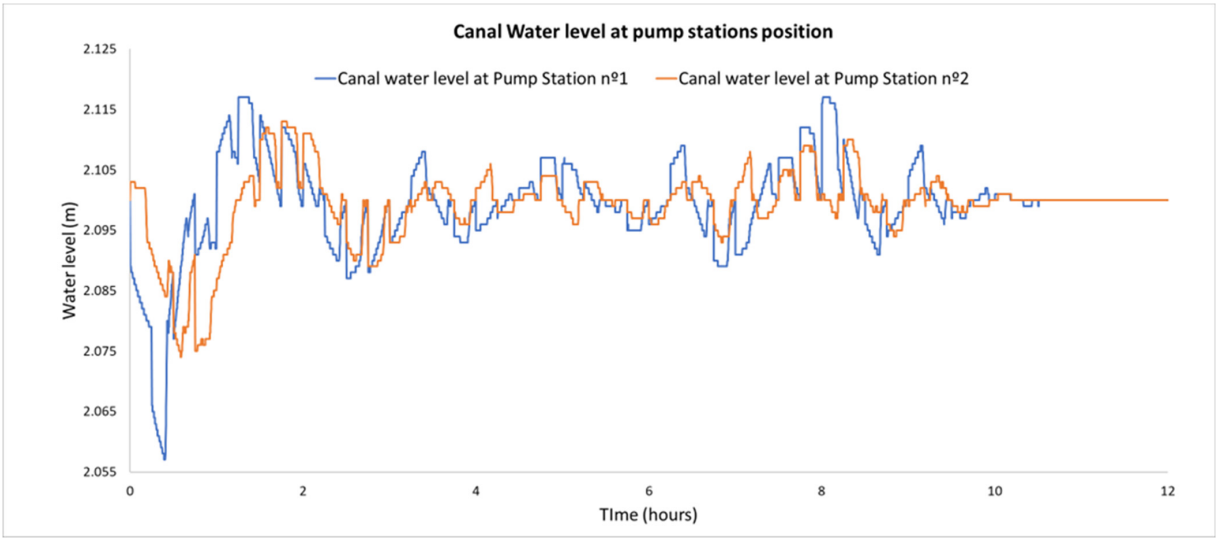


Figure 18. Water level at target points 1 (pump station n°1 location) and 2 (pump station n°2 location) in scenario II.

In the case of the OPF algorithm not being applied in scenario II, it would be difficult to estimate the optimal pumping flow trajectories due to the complexity of this scenario. In this specific scenario, pump stations would only operate in the case of water level at the reservoirs decreasing so much and water level prediction at reservoirs being below 1 m.c.a. during the time horizon. This new version of scenario II has been proposed in order to compare with the last version of scenario II. The results of this new version of scenario II are shown in Figures 19 and 20.

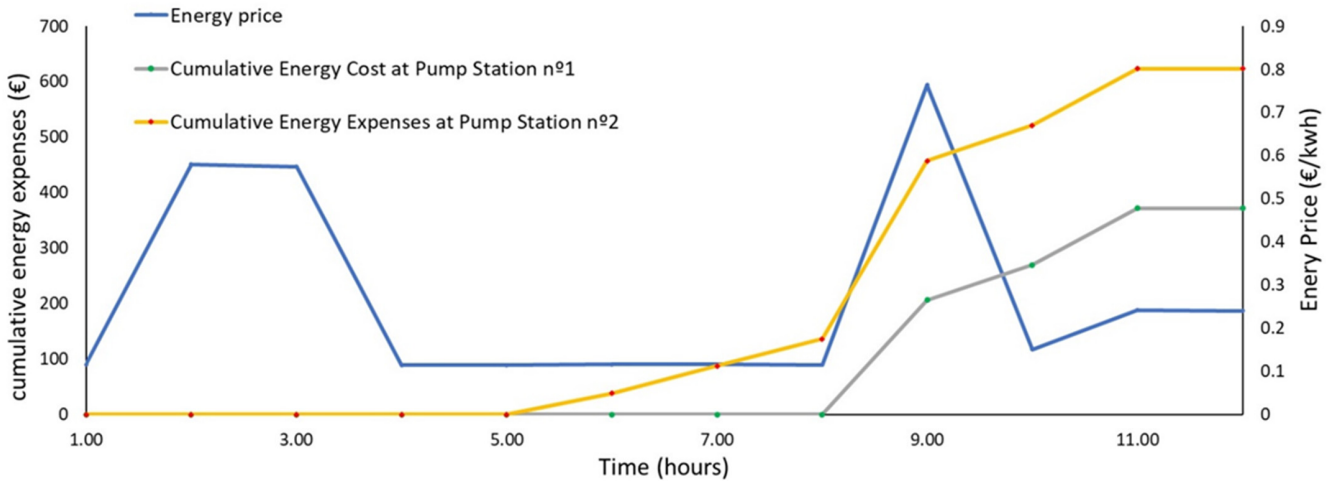


Figure 19. The energy price vs. cumulative energy expenses at pump stations n°1 and n°2 in scenario II (new version).

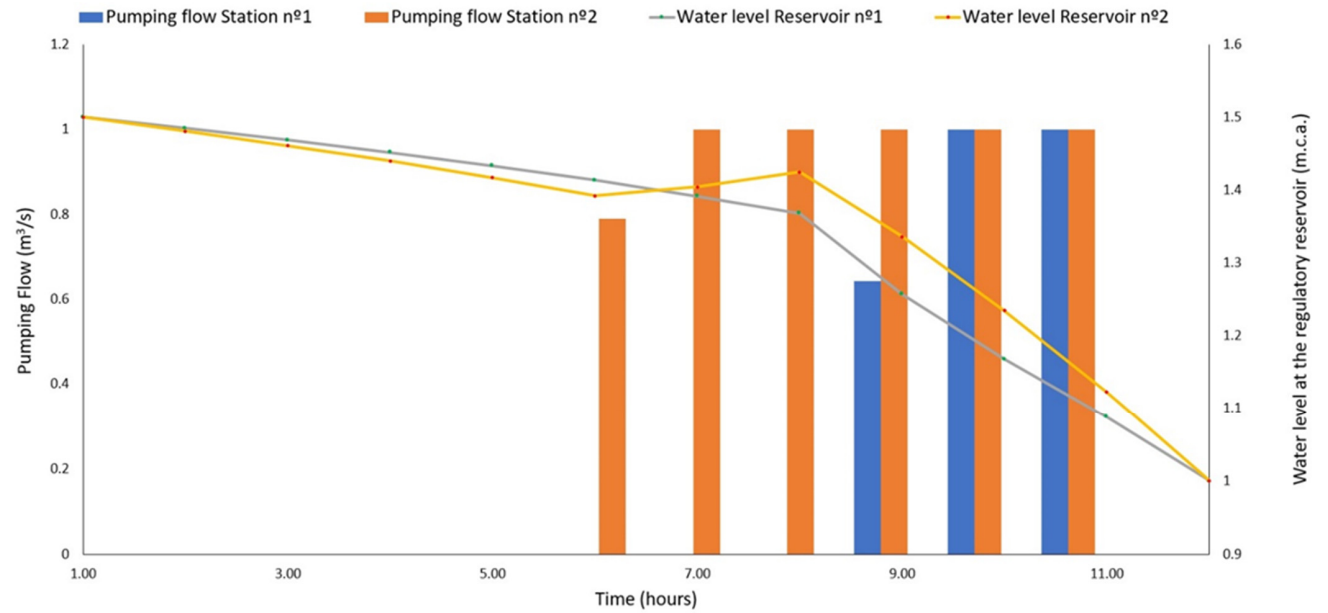


Figure 20. Pumping flow at stations n°1 and n°2 vs. water level at regulatory reservoirs n°1 and n°2 in scenario II (new version).

If we compare the first and second versions of scenario II, we can conclude that the OPF algorithm is able to reduce the cumulative energy expenses by a percentage of 58%, which is a huge amount of money in just 12 h.

4. Conclusions

The pumping flow trajectory is an essential parameter to operate a pumping station. Not using tools such as the OPF algorithm can increase the energy expense and

consumption at the pumping station, as well as reduce the competitiveness of the irrigation system and farmers. Nowadays, the agriculture margins are so low that considering the optimization of pumping flow trajectories should be mandatory for a watermaster.

The OPF algorithm is formulated regarding the energy and mass conservation equation and applying particular constraints associated with the water infrastructure. The OPF algorithm estimates the optimum pumping flow trajectory in order to reduce energy expenses regarding crop flow demand as well as energy consumption.

The OPF solves an optimization problem using the SLSQP method (sequential least square programming), which is implemented as a constrained non-linear optimization problem using a robust method with a fast convergence rate in comparison to other methods such as Nelder–Mead or Powell.

Two different scenarios were proposed to test the OPF algorithm. Scenario I was proposed to assess the logic of the algorithm's control when operating a pump station in an irrigation system, as well as to evaluate the algorithm's robustness and sensitivity. Instead, scenario II was proposed to test OPF together with the GoRoSo algorithm in order to check the good performance of the overall control diagram considering a test case based on the ASCE test cases.

The first scenario showed us that OPF calculated the optimal pumping flow trajectories according to the energy price during off-peak time periods, which was possible as crop water demand could be supplied just by pumping during those periods with reservoir support. On the other hand, the algorithm always respects the requirements of equality and inequality constraints, i.e., the water level of the reservoir of over 1 m.c.a. and the pumping flow from 0 to 25 m^3/h in scenario I.

The second scenario was developed considering two versions. In the first one, it is quite interesting to look at the algorithm's synchronisation because GoRoSo and OPF have to keep the water levels constant at the target points in the canal and provide crop flow demands from the reservoir during the time horizon. The result shows us the complexity of estimating the best solution in the case of a multiparameter optimization problem. In scenario II, the OPF algorithm also considered a price energy per hour to estimate optimal pumping flow trajectories, but pumping station n°2 operated when the water level reservoir was close to 1.5 m.c.a. (4–8 h), increasing the water level to 1.6 m.c.a. This happened because the energy price was cheaper during the first hours and the crop water demand was going to increase a lot during the next hours when energy price was more expensive. On the other hand, the GoRoSo algorithm had to prepare the irrigation canal state (water level at the target point) for the new boundary conditions (pumping flow) over the next hours. In addition, the irrigation canal opened gate number 0 and closed gate number 2, as the water level was expected to decrease at target point number 2 during the first hour because the pumping station started to operate. In the second version of scenario II, the GoRoSo algorithm worked without the OPF algorithm, so pump stations were only operating in the case of water level prediction at the reservoir decreasing below 1 m.c.a. during the time horizon. Comparing both versions, the OPF algorithm was able to reduce the cumulative energy expenses by 58%.

In light of the results obtained, the optimal pumping flow (OPF algorithm) is shown to be a competent and robust algorithm for the estimation of optimal pumping flow trajectories. Subsequently, its implementation in the overall control scheme of irrigation canals (offline computation module) was mandatory.

On the other hand, the overall control diagram of irrigation canals, including OPF algorithms, has operational limitations, which are evident in the manuscript, and future prospects aim to improve both. For instance, the OPF algorithm could be also implemented in the real-time module to improve energy expenses in real-time. On the other hand, the OPF algorithm should be applicable in cases of non-fully rough turbulent flow, along with upgrades considering various pump station configurations, introducing different characteristic curves of centrifugal pumps, water losses, and configurations of serial or parallel pumps.

Author Contributions: All authors contributed to the study's conception and design. Material preparation, data collection and analysis were performed by E.B. and M.T.Y. The first draft of the manuscript was written by E.B. and M.T.Y. and both authors read and approved the final manuscript. All authors have read and agreed to the published version of the manuscript.

Funding: The authors declare that no funds, grants, or other support were received during the preparation of this manuscript.

Institutional Review Board Statement: This material is the authors' own original work, which has not been previously published elsewhere. The paper is not currently being considered for publication elsewhere. The paper reflects the authors' own research and analysis in a truthful and complete manner. The paper properly credits the meaningful contributions of co-authors. The results are appropriately placed in the context of prior and existing research. All sources used are properly disclosed (correct citation). Literal copying of text must be indicated as such by using quotation marks and giving proper references. All authors have been personally and actively involved in substantial work leading to the paper and will take public responsibility for its content. (The author and co-author approve it. Enrique Bonet and Maria Teresa Yubero (12 March 2024)).

Informed Consent Statement: Informed consent was obtained from all individual participants included in the study.

Data Availability Statement: All data underlying the results are available as part of the article and no additional source data are required. If any reviewer needs additional data or documents, they can be delivered.

Conflicts of Interest: The authors declare no conflicts of interest.

Nomenclature

A(y)	The area of the wet section which depends on the water level "y"
ASCE	American Society of Civil Engineers
c	The gate width;
CSE	Canal Survey Estimation algorithm
bj	The j-gate width
f(x)	Objective function
ρ	Density
$E_{expenses}$	Energy expenses during horizon time period
$E_{minimum}$	Minimum energy expenses trajectory
E_{price}	Energy price during the horizon time of period
ET_0	Reference evapotranspiration per tree
ET_c	Crop evapotranspiration per tree
f	Darcy Weisbach coefficient
FCA	Friction Coefficient Algorithm
g	Gravity
GoRoSo	Gómez Rodellar Soler
GoRoSoBo	Gómez Rodellar Soler Bonet
g(x)	Equality constraints equations
h(x)	Inequality constraints equations
$H_{reservoir}$	Water level at the reservoir
H_b	Pumping head
H_{max}	Maximum water level at the reservoir
H_{min}	Minimum water level at the reservoir
$h_{pumping\ height}$	Height among water surface at irrigation canal regulatory reservoir
H_{total}	Total height among irrigation canal bottom and regulatory reservoir water level
IEC	International Energy Agency
J(E)	Residual function
K_c	Dimensionless parameter depending on the type of crop and period of the year
λ	Lagrange multipliers
mp	Number of pump stations
mc	Number of types of crops
n	Manning coefficient

nc	Number of checkpoints
np	Number of pools
L	Pipe length
OPF	Optimal pumping flow
Φ	Pipe diameter
P_i	Pressure at section "i"
P_t	Pump power
$Q_{crop\ demand}$	Crop flow demand trajectory
Q_{max}	Maximum flow value
$Q_{pumping}$	Pumping flow trajectory
$q_{offtake}$	Discharge through the orifice offtake
$Q_{reservoir\ outlet}$	Discharge from regulatory reservoir to the crop
q_s	Discharge through the lateral spillway
σ	Lagrange Multipliers
s(x)	Function "s" evaluated at the "x" solution
S(y)	Horizontal surface of the reception area in the checkpoint
SQP	Sequential Quadratic Problem
T	Operational time step
T_a	Width of the wall of a reservoir
u	The open gate height
UNESCO	Nations Educational, Scientific and Cultural Organization
U_R	Reference gate trajectories
vi(k)	Mean velocity at time instant k at canal section i
γ	Specific weight
Y	Canal water level at pump station location
y(k)	Subset of water depths of the state vector at time instant k at checkpoints
Y_M	Measured water level at target points
Y*	Desired water level at target points
yi(k)	Water depth at time instant k at canal section i
y_o	Height of the center of the orifice from bottom of the gravity offtake
z	Elevation of the section studied above the reference plane
$\nabla^2 L$	Laplacian operator
ΔH_R	Distributed water losses in a pipe
ΔM	Reservoir mass variation between time steps
Δt	Numerical time step
Δx	Numerical discretization of a variable x

References

1. Aguilar, J.V.; Langarita, P.; Rodellar, J.; Linares, L.; Horváth, K. Predictive control of irrigation canals—Robust design and real-time implementation. *Water Resour. Manag.* **2016**, *11*, 3829–3843. [CrossRef]
2. Alizadeh, M.R.; Ehsani, A.H.; Omid, M.; Makui, A. Optimal operation of pumping stations in irrigation networks. *J. Irrig. Drain. Eng.* **2003**, *129*, 104–112.
3. Bohórqueza, J.; Saldarriaga, J.; Vallejoa, D. Pumping pattern optimization in order to reduce WDS operation costs. In Proceedings of the 13th Computer Control for Water Industry Conference, CCWI 2015, Leicester, UK, 2–4 September 2015. [CrossRef]
4. Bonet, E. Experimental Design and Verification of a Centralize Controller for Irrigation Canals. Ph.D. Thesis, UPC (Technical University of Catalonia), Barcelona, Spain, 2015.
5. Bonet, E.; Gómez, M.; Soler, J.; Yubero, M.T. CSE algorithm: 'Canal Survey Estimation' to evaluate the flow rate extractions and hydraulic state in irrigation canals. *J. Hydroinformatics* **2017**, *19*, 62–80. [CrossRef]
6. Bonet, E.; Gómez, M.; Yubero, M.T.; Fernández-Francos, J. GoRoSoBo: An overall control diagram to improve the efficiency of water transport systems in real time. *J. Hydroinformatics* **2017**, *19*, 364–384. [CrossRef]
7. Bonet, E.; Russo, B.; González, R.; Yubero, M.T.; Gómez, M.; Martí Sánchez, J. The FC Algorithm to Estimate the Manning's Roughness Coefficients of Irrigation Canals. *J. Agric.* **2023**, *13*, 1351. [CrossRef]
8. Clemmens, A.J.; Kacerek, T.F.; Grawitz, B.; Schuurmans, W. Test cases for canal control algorithms. *J. Irrig. Drain. Eng.* **1998**, *124*, 23–30. [CrossRef]
9. Clemmens, A.J.; Bautista, E.; Wahlin, B.T.; Strand, R.J. Simulation of automatic canal control systems. *J. Irrig. Drain. Eng.* **2005**, *131*, 324–335. [CrossRef]
10. Coon, W.F. *Estimation of Roughness Coefficients for Natural Stream Channels with Vegetated Banks*; Technical Report, U.S Geological Survey Water-Supply Paper No. 2441; UAGS: Reston, VA, USA, 1998.

11. Egito, T.; Azevedo, J.; De Tarso, S. Optimization of the operation of water distribution systems with emphasis on the joint optimization of pumps and reservoirs. *Water Supply* **2023**, *23*, 1094–1105. [CrossRef]
12. United States Geological Survey. Where Is Earth's Water? 2016. Available online: https://www.usgs.gov/media/images/distribution-water-and-above-earth-0 (accessed on 13 May 2020).
13. International Energy Agency. Spain 2021 Energy Policy Review. 2021. Available online: https://iea.blob.core.windows.net/assets/2f405ae0-4617-4e16-884c-7956d1945f64/Spain2021.pdf (accessed on 12 October 2023).
14. Khwaja, S.A.; Tung, Y.K. Pump scheduling for water distribution systems using genetic algorithms. *J. Water Resour. Plan. Manag.* **1999**, *125*, 209–216.
15. Ormsbee, L.E.; Reddy, S.L. Pumping System Control Using Genetic Optimization and Neural Networks. *IFAC Proc. Vol.* **1995**, *28*, 685–690. [CrossRef]
16. Litrico, X.; Fromion, V.; Baume, J.-P.; Arranja, C.; Rijo, M. Experimental validation of a methodology to control irrigation canals based on Saint-Venant equations. *Control Eng. Pract.* **2005**, *13*, 1425–1437. [CrossRef]
17. McCormick, G.; Powell, A.R.S. Optimal Pump Scheduling in Water Supply Systems with Maximum Demand Charges. *J. Water Resour. Plan. Manag.* **2003**, *129*. [CrossRef]
18. Müller, T.M.; Leise, P.; Lorenz, I.S.; Altherr, L.C.; Pelz, P.F. Optimization and validation of pumping system design and operation for water supply in high-rise buildings. *Optim. Eng.* **2021**, *22*, 643–686. [CrossRef]
19. Peña, J.I. A note on hydropower as a marginal price setter for Spain's electricity market in 2021–2022. *J. Util. Policy* **2024**, *87*, 101726. [CrossRef]
20. Reis, A.L.; Lopes, M.A.R.; Andrade-Campos, A.; Henggeler Antunes, C. A review of operational control strategies in water supply systems for energy and cost efficiency. *J. Renew. Sustain. Energy Rev.* **2023**, *175*, 113140. [CrossRef]
21. Romano, G.; Baiani, S.; Mancini, F.; Tucci, F. Reducing CO_2 Emissions and Improving Water Resource Circularity by Optimizing Energy Efficiency in Buildings. *Sustainability* **2023**, *15*, 13050. [CrossRef]
22. Salimi, S.; Almuktar, S.A.A.A.N.; Scholz, M. Impact of climate change on wetland ecosystems: A critical review of experimental wetlands. *J. Environ. Manag.* **2021**, *286*, 112160. [CrossRef] [PubMed]
23. Smith, M.; Allen, R.G.; Pereira, L.S.; Raes, D. *Crop Evapotranspiration—Guidelines for Computing Crop Water Requirements*; FAO Irrigation and Drainage Paper 56; FAO: Rome, Italy, 1990; Volume 139, pp. 41–54. ISBN 92-5-104219-5. [CrossRef]
24. Soler, J.; Gómez, M.; Rodellar, J.; Gamazo, P. Application of the GoRoSo Feedforward Algorithm to Compute the Gate Trajectories for a Quick Canal Closing in the Case of an Emergency. *J. Irrig. Drain. Eng.* **2013**, *139*. [CrossRef]
25. UNESCO. The United Nations World Water Development Report 2020: Water and Climate Change, Executive Summary. Technical Report. 2020. Available online: https://unesdoc.unesco.org/ark:/48223/pf0000372882 (accessed on 8 August 2023).
26. United Nations. *World Population Prospects: The 2015 Revision, Key Findings and Advance Tables*; Technical Report; United Nations: Geneva, Switzerland, 2015.
27. Wahlin, B.T.; Clemmens Albert, J. Automatic Downstream Water-Level Feedback Control of Branching Canal Networks: Simulation Results. *J. Irrig. Drain. Eng.* **2006**, *132*, 208–219. [CrossRef]

Disclaimer/Publisher's Note: The statements, opinions and data contained in all publications are solely those of the individual author(s) and contributor(s) and not of MDPI and/or the editor(s). MDPI and/or the editor(s) disclaim responsibility for any injury to people or property resulting from any ideas, methods, instructions or products referred to in the content.